IEEE Access
Multidisciplinary | Rapid Review | Open Access Journal

Received January 15, 2021, accepted January 25, 2021, date of publication January 28, 2021, date of current version February 10, 2021.

Digital Object Identifier 10.1109/ACCESS.2021.3055221

Laser Speckle Integrated Multispectral Imaging System for *In-Vivo* Assessment of Diabetic Foot Ulcer Healing: A Clinical Study

SHEENA PUNAI PHILIMON[1], (Member, IEEE), AND AUDREY KAH CHING HUONG[2], (Senior Member, IEEE)

[1]Faculty of Engineering, Computing and Science, Swinburne University of Technology at Sarawak, Kuching 93350, Malaysia
[2]Department of Electronic Engineering, Faculty of Electrical and Electronic Engineering, Universiti Tun Hussein Onn Malaysia, Batu Pahat 86400, Malaysia

Corresponding author: Audrey Kah Ching Huong (audrey@uthm.edu.my)

This work was supported by the Ministry of Higher Education Malaysia (MOHE) through Fundamental Research Grant Scheme (FRGS/1/2020/TK0/UTHM/02/27). We also acknowledge a partial support of the publication fee by the registrar office of Universiti Tun Hussein Onn Malaysia (UTHM).

ABSTRACT The high prevalence of the world's population diagnosed with diabetes mellitus, with a significant number suffering from diabetic foot ulcer (DFU), has always been a global concern over the years. The rapid rise of this disease in the last decades is deemed increasingly alarming as it has left deleterious effects not only on affected patients but also on the society and nation. This paper aims to develop a reliable diagnostic tool to address the tremendous need for coordinated and efficient DFU management via prediction of transcutaneous oxygen saturation (S_tO_2) and relative blood perfusion (τ) in the affected limb. This system integrates the use of a multispectral imaging and laser speckle contrast imaging technique for two-dimensional (2D) mapping of tissue oxygen and blood perfusion level in ulcerated foot. Longitudinal study revealed a slightly higher mean S_tO_2 and τ level in healed ulcer than in impaired healing, despite the data indicating no statistical significance between these two groups ($p-$ value > 0.05). It was observed that a mean S_tO_2 of at least 70 % and τ value of 1.5 ($\times 10^3$) are necessary during the proliferative phase to ensure progressive healing. Based on these findings, this study concluded that high tissue oxygenation and perfusion levels are pivotal to ensure progressive wound healing. This work provides a rationale for evaluating the healing outcomes of skin grafting procedures in diabetic ulcers based on observation of quantitative changes in blood perfusion and tissue oxygen level during its revascularization phase.

INDEX TERMS Biomedical signal processing, diabetic foot ulcer, laser speckle contrast imaging, multispectral imaging.

I. INTRODUCTION

A retrospective study by the World Health Organization (WHO) based on data sources collected from 221 countries and territories estimated at least 451 million adults aged $18-99$ years old worldwide diagnosed with diabetes mellitus as of the year 2017 [1]. This number was projected to increase to 693 million by the year 2045. A majority of diabetes cases were identified among those living in low- and middle- income countries, with Western Pacific region having the highest prevalence of total global diabetes population. China was quoted as having the highest number of population with diabetes with 98.4 million adults diagnosed, followed by India with 65.1 million [2]. Specifically, a retrospective study by Raja [3] stated that diabetic foot ulcer (DFU), a microvascular complication of diabetes mellitus, constituted 15 % of all diabetes cases. Of this figure, approximately 20 % of DFU cases are the results of peripheral and autonomic neuropathy as well as diabetic angiopathy, which if left untreated, can lead to foot infection and amputation of the lower extremity. In addition, diabetes mellitus has also been cited as one of the major contributors of chronic kidney disease (CKD) that can lead to fatality [4]. Socio-economic status, living environment and eating habits are among the factors linked to the rise in diabetes cases worldwide [5]. The global health expenditure for diabetes patients in 2017 was estimated to be USD 850 billion, which was twice the expenditure of patients without diabetes [1]. Hence, there is an increasing demand

The associate editor coordinating the review of this manuscript and approving it for publication was Filbert Juwono.

for coordinated and efficient wound healing management in DFU patients nationwide.

The predominance of DFU among patients suffering from diabetes mellitus has led to limitations in daily activities as well as reduced living quality. The call for proper management and assessment of chronic diabetic wound is necessary following the increase in the regular visits of healthcare centers and hospitals by the patients. As the economy continues to decline and the cost of medical fee increases, the need for a more cost-effective and systematic chronic wound management solution expands throughout the nation [6]–[8]. This was based on evidence-based global consensus recommendations on prevention and management of foot problems in diabetes in [6]. There are many medical options for *in-vivo* assessment of DFU such as the photoacoustic imaging technique [9], positron emission tomography (PET), computed tomography (CT) and functional magnetic resonance imaging (fMRI) [10]. While most of these methods are able to provide the information needed, their limitations are of great concern. This includes the reading and interpretation of medical images that can be tedious and time consuming, and the requirements of the scan that are deemed unsuitable to be used on certain individuals (e.g. patients with claustrophobia, pacemaker or magnetized metal implantation) in the case of fMRI. PET/CT could be a better alternative for patients with metal implants. But the main issue concerning the use of PET/CT for this purpose is the administration of glucose analogue as metabolic tracer [11]. Since this examination measures changes in glucose uptake in patients, the subject's blood sugar level would first be assessed before the tracer is injected, making the examination process cumbersome and inefficient. This modality is commonly used as the reference standard for diagnosis of bone infection, the usefulness of PET/CT in monitoring of diabetic foot infection remains unclear [11], [12]. It should be mentioned that the use of the above mentioned techniques solitarily is unable to concurrently provide information of blood flow and tissue oxygenation status, let alone their cost effectiveness, practicability and availability for routine screening at different phases of DFU healing progress. Because of the advantages and disadvantages to each existing modalities, multimodal imaging was suggested as better alternative for DFU monitoring. Earlier works by [13] and [14] demonstrated the possibilities of simultaneously measuring blood flow and oxygenation using photoacoustic Doppler on animals (i.e. bovine, mouse and chicken). Despite the promising results, its translation to clinical practice remains challenging due to the limitation in the experimental design (that sometimes require the use of a contrast agent [15]) for application on intact human skin. There exists a gap for a non-invasive and dye-free approach to determine microcirculation in human skin tissue [16]. Although recent works attempted to employ photoacoustic imaging for routine examination of the healing of chronic ulcers, these works focused on either blood circulation associated with leaking vessels [9] or quantification of blood oxygenation [17].

Accurate wound healing assessment should include physical examination, microcirculatory functional assessment and a complete understanding of wound pathology. Laser speckle contrast technique was reported able to provide measurement of cutaneous blood flow and tissue perfusion [18]–[20], whereas spectroscopy imaging is a non-invasive approach to acquire optical properties of human tissue, which signals may be processed to provide tissue oxygen level [21]–[24]. Even though earlier studies [25], [26] mentioned a strong correlation between blood flow perfusion and tissue oxygenation to be expected during different phases of healing, no work has, thus far, combined the technology of these two measurements.

In view of this, an approach combining laser speckle and multispectral imaging systems is adopted here for sequential measurement of tissue oxygenation and blood perfusion level in positive and impaired healing diabetic ulcers. It is hypothesized that tissue microcirculatory activities are key determinants of wound healing, and increased blood perfusion and oxygen supply to wound regions are likely to guarantee positive healing progress. It is hoped that this proposed strategy can assist healthcare professionals in medical/surgical decision-making process (e.g. the need of amputation) through complementary information of regions with poor perfusion and oxygen level. The rest of this paper is organized as follows. In Section II, we introduce the laser speckle incorporated multispectral imaging system, the formulas for tissue perfusion and oxygen level estimation, and selection of participants in this study. This is followed by results and discussions based on two groups of wound healing, using microcirculatory parameters of healthy subjects as reference, in section III and IV. Lastly, the final section gives an overall conclusion and recommendations for future research.

II. RESEARCH METHOD

The development of the integrated imaging system was generally divided into two major stages, namely laser speckle contrast and multispectral imaging for measurement of blood flow perfusion and tissue oxygenation, respectively. This study was carried out on healthy control subjects and DFU patients. These investigations are important to validate the performance of the system, and for understanding the function and response of microcirculatory variables in wound healing. The reported variables' range can be used as an assessment reference in clinical settings to evaluate the effectiveness of prescribed treatments on foot ulcer recovery process.

A. LASER SPECKLE INCORPORATED MULTISPECTRAL IMAGING SYSTEM

A schematic arrangement of the incorporated imaging system is shown in Fig. 1. All measurements were performed in reflection mode. The laser speckle contrast imaging system comprised of a low power laser diode of wavelength, $\lambda = 650$ nm (product code LD-650nm, 5 mW), which was placed

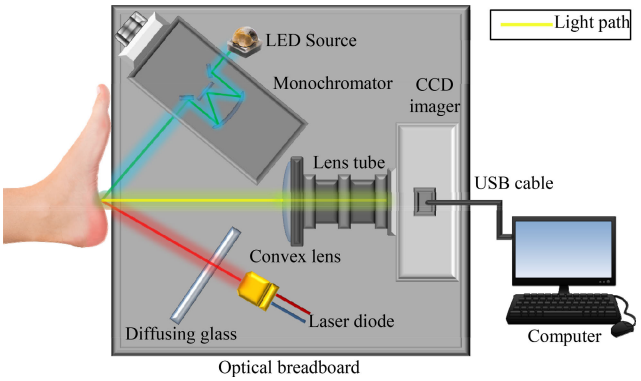

FIGURE 1. Schematic diagram of laser speckle incorporated multispectral imaging system mounted on an optical breadboard.

at a distance of 140 mm from the targeted skin surface and an angle of approximately 45 ° from normal to reduce the effects of specular reflection. A diffusing glass was placed at the center of the illumination plane to generate homogenous illumination of samples.

The detection system consisted of a plano-convex lens to focus light reflected from the targeted site onto a charge-coupled detector (CCD) (BUC4-500C Cooled CCD Digital Camera from BestScope) controlled using ISCapture imaging software (V3.5 by Tucsen Photonics). The imager field of view (FOV) is given by 5 mm × 7 mm. The CCD integration time was set at 10 seconds to achieve an optimal signal-to-noise ratio (SNR) of 30 dB. The 12-bit raw images were saved and transferred to a personal computer via a universal serial bus (USB) data transfer cable for offline post-processing. The optical lens was placed at normal from the skin surface in front of the CCD imager; the latter positioned at 200 mm from the skin. Two convex lenses in a lens tube in front of the CCD imager were arranged in tandem manner to achieve a magnification value, $M = 1.0$. This configuration was specifically chosen in order to give a speckle size value, S, of approximately one pixel using the following expression [27]:

$$S = 1.22\lambda NM \tag{1}$$

where f-number, N, is expressed as the ratio of effective focal length, f_L, to the aperture diameter, D. Here, the f-number is calculated as 4.55.

The multispectral imaging system comprises of a high-intensity white LED (XLamp® XQ-E LED from Cree) and a monochromator (Oriel Mini Monochromator part no. 78026 from Newport) with a built-in diffraction grating to produce light in the visible wavelength range of 300 − 800 nm. In this study, we used light of wavelength 530 − 570 nm at a 10 nm interval. However, this type of measurement is susceptible to specular glare from the surface of the measurement subject (in the detection). For this reason, both the monochromator and laser diode were placed opposite each other on either side of the detector; the angle of these illumination source position was approximately 45 ° from normal and a distance of 130 mm

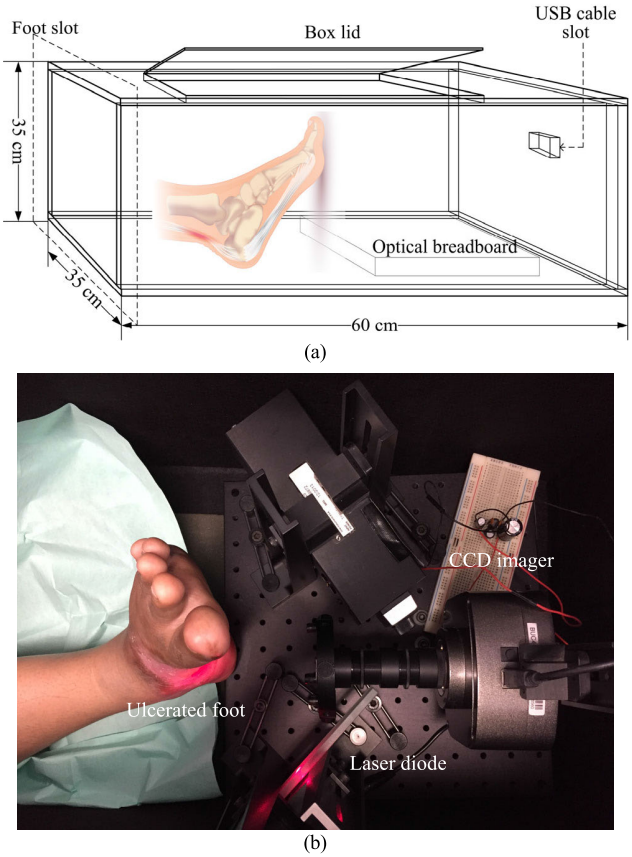

FIGURE 2. Diagram of the experimental chamber designed for DFU perfusion and oxygen saturation measurement (a) and an example of the affected limb placed inside the measurement chamber (b).

from the skin surface. The light penetration depth in skin tissue for the considered wavelengths of incident light is approximately 5 mm [28].

These experimental setups were mounted on an optical breadboard and placed inside an enclosed black box of dimensions 60 cm × 35 cm × 35 cm (Length × Height × Width) to provide a total darkness condition. A diagram of the designed box that accommodates both the system and investigated limb is shown in Fig. 2(a). The investigated limb would be placed inside the box against a light absorbing black-out material as shown in Fig. 2(b). The interior of the box was covered with black flock paper to minimize reflection during measurement. During the experiment, the chamber was placed on a portable trolley for better system mobility while the subject was rested on the bed. Each subject was instructed to sit in a relaxed position with the ulcerated foot placed inside the enclosed black box as demonstrated and to remain still throughout measurement to reduce motion artefact. They were first acclimatized to a controlled room temperature set at 20 °C for at least fifteen minutes prior to measurement. It must be mentioned that some of the ulcers considered in this study were not located on the plantar surface of the foot, but ample space is available to allow adjustments of foot placement according to the patients' comfort.

B. BLOOD PERFUSION MEASUREMENT

The prediction of blood perfusion involved two main steps. First is the calculation of the speckle contrast value, k, which is defined as the ratio of standard deviation, σ, to the mean of the measured intensity, $\langle I \rangle$, given by [29]:

$$k = \frac{\sigma}{\langle I \rangle} = \frac{\sqrt{\frac{\sum_{i=1} (I_i - \langle I \rangle)}{N-1}}}{\langle I \rangle} \tag{2}$$

where I is the time-integrated intensity measurement and N is sliding window size given by 49 (corresponding to 7×7 pixels window) chosen following the report of [30].

The k value can be expressed as a function of correlation time, τ in (3) [31]. The latter is normally taken as the relative estimation of blood flow or the time taken for the contrast to drop to a specific level.

$$k\left(T_s, \tau\right) = \left(\beta \frac{\exp\left(-2\left(T_s/\tau\right)\right) - 1 + 2\left(T_s/\tau\right)}{2\left(T_s/\tau\right)^2}\right)^{1/2}. \tag{3}$$

Here, parameter T_s is defined as the exposure time of the CCD imager and is given by $T_s = 10$ seconds. Parameter β is a constant that constitutes speckle averaging, which value is taken to be equal to one following the report in [29]. Based on the k value calculated from (2), the unknown τ value in (3) was determined using a non-linear fitting function (fminsearch) available in MATLAB® (MathWorks, Inc.).

In this work, blood flow is specifically referred to as perfusion and it is a measurement of magnitude acknowledged as the arbitrary "perfusion unit" [32].

C. TISSUE OXYGEN MEASUREMENT

The estimation of transcutaneous blood oxygen saturation, S_tO_2, in this work was using a prediction model known as the Extended Modified Lambert Beer (EMLB) developed in [33]. This model is extended from the MLB law initially proposed by Duling and Pittman [34] shown here in (4). The good performance of EMLB model was observed in [33] using Monte Carlo method with excellent agreement between the predicted and ground truth values. The MLB law in (5) represents a linear relationship between the light attenuation, A, and light absorption, μ_a, of a given medium with parameter d taken as the "light pathlength". An offset, represented by G, is regarded as an estimation of attenuation due to scattering.

$$A\left(\lambda\right) = G + \mu_a d. \tag{4}$$

The μ_a in (4) can be expressed as a function of the extinction coefficient of oxyhemoglobin $\left(\varepsilon_{HbO_2}\right)$ and deoxyhemoglobin (ε_{Hb}) as follows:

$$\mu_a\left(\lambda\right) = \varepsilon_{HbO_2} C_{HbO_2} + \varepsilon_{Hb} C_{Hb} \tag{5}$$

where C_{HbO_2} and C_{Hb} represent concentration of oxyhemoglobin and deoxyhemoglobin, respectively. Expressing light attenuation as a function of S_tO_2 gives (6) with $\Delta\varepsilon$ representing $\varepsilon_{HbO_2}\left(\lambda\right) - \varepsilon_{Hb}\left(\lambda\right)$ [33]:

$$A\left(\lambda\right) = G_0 + \left(\Delta\varepsilon S_tO_2 + \varepsilon_{Hb}\left(\lambda\right)\right) d_0 T + G_1\lambda + \lambda \exp\left(-\left(\Delta\varepsilon S_tO_2 + \varepsilon_{Hb}\left(\lambda\right)\right) d_1 T\right) \tag{6}$$

where the attenuation offset, G_0, scattering and absorption dependent offset, $G_1\lambda$, S_tO_2 and mean light pathlengths related parameters, d_0 and $d_1\lambda$, are unknowns. Their values must be determined. A more detailed explanation and use of this equation can be found in [33]. The value of these unknowns is to be found to give the best fit of the calculated spectrum to the experimental data.

The MATLAB *fminsearch* function uses Nelder-Mead simplex algorithm [35], an unconstrained non-linear optimization algorithm to search for the most probable unknown values. This algorithm employs a simplex of $n + 1$ for an n-dimensional vector x, with the assumption that n is the length of x. The *fminsearch* function will seek for the minimum scalar function of the variable, starting with the assigned arbitrarily selected value of '1'. If large mean difference in the calculated and measured attenuation magnitudes is calculated, i.e. $\Delta E > 1 \times 10^{-20}$, this process would continue to seek a new value to each fitting parameter. With every new value assigned, the attenuation values are recalculated form (6) until $\Delta E \leq 1 \times 10^{-20}$ or the number of iteration has exceeded 1000, where the optimal τ and S_tO_2 values are assumed to have been achieved. The ΔE and iteration limit were arbitrarily selected following previous related work [36] who revealed that these values are sufficient for the convergence of the calculated attenuation spectrum, A_c, to that of the measured spectrum. An increase in the number of iterations or decrease in the ΔE limit would result in an improved accuracy of the estimated value, although this would inadvertently result in an increased computation time.

D. SUBJECTS

Patients with DFU were recruited from the outpatient clinic at the Orthopedic Department, Hospital Sultanah Nora Ismail (HSNI), Johor, Malaysia. Ethical approval for this single center study was obtained from the Medical Research and Ethics Committee (MREC), Ministry of Health Malaysia (NMRR-16-2475-33611 (IIR)). These recruits were adult Type 2 diabetes patients aged 18 years old and older with newly developed or ongoing ulcers at locations near the foot plantar. Exclusion criteria included subjects who are pregnant at the time of the study, and those with either past medical history of hypertension or underlying medical illnesses (such as heart disease and cancer) that might affect the reading. The participation was voluntary and the selected subjects were asked to fill in an informed consent prior to the experiment. The clinical study was performed over a duration of two years (March 2017 – March 2019).

Meanwhile prior to the commencement of this research study, the feasibility of this system was verified using measurement results from experiments on fifteen healthy control

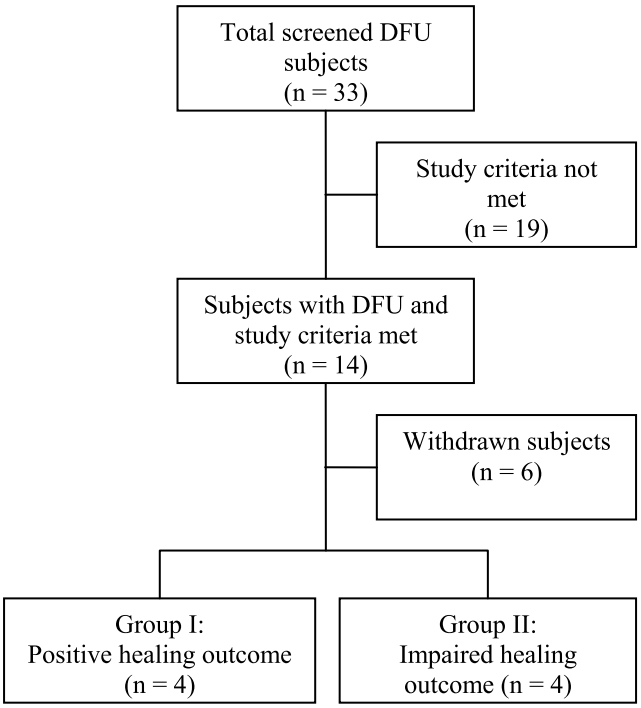

FIGURE 3. Consort diagram of subjects enrolled in this study.

subjects aged between 24 – 29 years old. These subjects were of Asian origins. They are students at Universiti Tun Hussein Onn Malaysia (UTHM) during the time of the study. Experiments were conducted under two conditions: during at rest and arterial blood flow occlusion, to test the effectiveness of the system to detect changes in microcirculation. In the blood flow occlusion experiment, a cuff pressure of 140 mmHg was inflated around the upper left arm of the recruits for 60 seconds before the measurements. All measurements were taken from thenar region of their left palm.

III. RESULTS

The consort diagram of DFU subjects' recruitment is presented in Fig. 3. A total of thirty-three subjects were initially approached in this study. However, nineteen were excluded from the study for not meeting the criteria and six eligible subjects withdrew his or her consent to participate in this study. The final study sample approved for this research comprised of a total of eight Type 2 DFU subjects (six males and two females); four subjects with positive healing wound (three males and one female) and four subjects with impaired healing wound (three males and one female).

Details of DFU subjects in both groups are listed in Table 1. The data in this study are generally divided into two main groups, namely positive healing and impaired healing wounds that were yet to be discharged from the clinical follow-up (as of March 2019, the final day before the approval expired), based on the decision of the consulting physician. The routine follow-up visit for each subject is every two months or may be more depending on the severity and healing progress of the foot ulcers.

TABLE 1. Personal details and clinical status of the recruited DFU subjects.

Subject	Gender	Ulcer age (as of March 2019)	Group
001	Female	17 months	Positive healing
002	Male	8 months	
003	Male	14 months	
004	Male	10 months	
005	Male	26 months	Impaired healing
006	Male	20 months	
007	Female	16 months	
008	Male	7 months	

A. MICROCIRCULATORY RESULTS OF INVESTIGATED GROUPS

The system described in section II was used on healthy control subjects for measurement of blood perfusion and tissue oxygen during at rest and arterial blood occlusion conditions. The results from this experiment provide a benchmark for comparison with data obtained from the DFU subjects. A mean τ value of $2.87 \pm 1.35\ (\times 10^3)$ was recorded for at rest, and this value dropped to $1.23 \pm 0.58\ (\times 10^3)$ during arterial blood flow occlusion. Likewise, the results revealed mean S_tO_2 values of 72.44 ± 3.10 % during at rest that decreased to 71.25 ± 3.43 % under cuff occlusion. These mean τ and S_tO_2 d were compared using a two-tailed paired samples t-test analysis in SPSS software (IBM SPSS Statistics, Version 23) with 95 % confidence level. The results showed a statistically significant difference of $p \leq 0.05$ for different experiment conditions. Fig. 4 showed the median and quartile of τ and S_tO_2 for the measurements of control group under these conditions.

An example of S_tO_2 and τ values for a 5 cm × 7 cm area of the affected skin of a positive healing DFU over a period of nine months is shown in Fig. 5(b) and Fig. 5(c). The selected site is enclosed by the square frame in Fig. 5(a).

The S_tO_2 maps in Fig. 5(b) depict low spatial variability between pixels for measurements taken between August 2017 and April 2018, with an overall high percent S_tO_2 value above 70 % observed during this period. The S_tO_2 map recorded on April 2018 shows fluctuation in the values (i.e. ranging between 40 % and 50 % as shown in the blue colored circle) corresponds to keratinocytes at wound edges. These values are lower as compared to wound bed region with reddish granulation tissue that measures up to 80 % in S_tO_2. This difference in the range of S_tO_2 may be used as a qualitative indicator to differentiate dry and healed epithelial tissue from fresh granulation tissue. Meanwhile based on Fig. 5(c), the speckle maps appear equally distributed with considerably small differences between visits. The intensity of speckle contrast is reduced as the wound progressed toward healing. This trend of microcirculatory changes in the healed wound shows that these two parameters are correlated and the magnitude of changes is consistent throughout the healing period.

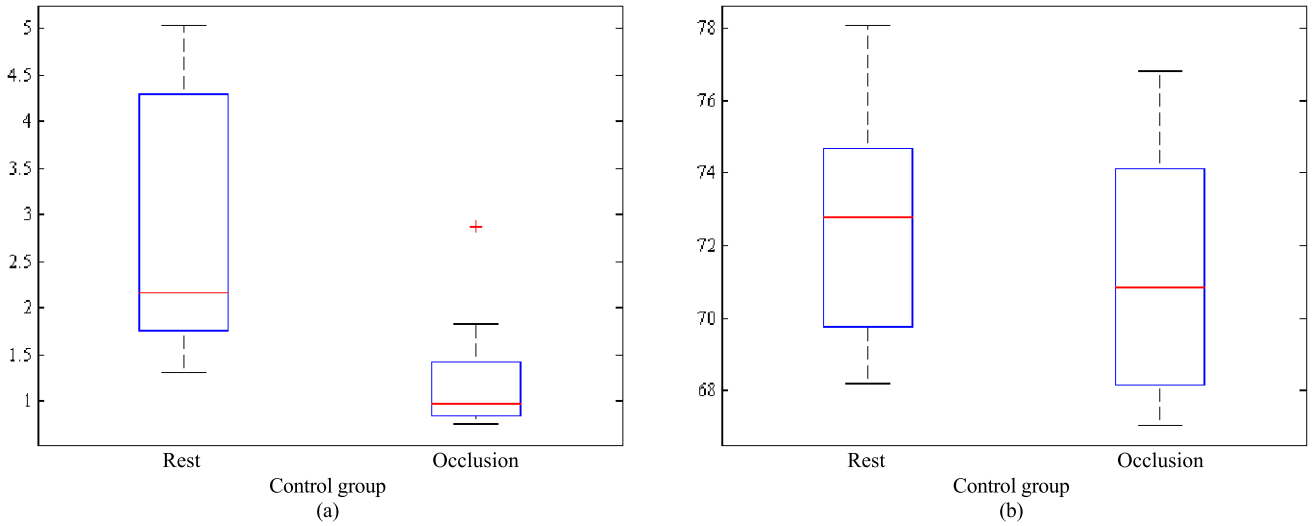

FIGURE 4. Comparison of box plot for calculated (a) blood perfusion, τ, and (b) tissue oxygen, S_tO_2, of control subjects during at rest and occlusion conditions. The median value of respective data sets is indicated by the red line in the center of the box plot.

Fig. 6 illustrates *in-vivo* changes in tissue perfusion versus the normalized number of clinical visits for comparison of blood perfusion and S_tO_2 trends between the positive and impaired healing diabetic wounds. In the positive healing wound group, most of these subjects (Subjects 001 and 002) showed similar trend in τ changes, with the values increased during mid-healing before gradually decreased in their final visit, which may indicate a blood perfusion level that has stabilized in healed wounds. An example of this can be referred to Subject 001, whose wound profile is shown in Fig. 5. Here, it can be seen how the S_tO_2 and τ dropped to a lower value of 67.36 ± 1.17 % and 0.65 ± 0.29 $(\times 10^3)$, respectively on the fourth day of visit. A possible reason for this could be the presence of migrating keratinocytes from the wound edge. Meanwhile in the impaired healing wound group the graph illustrates an unpredictable trend in τ values that fluctuated between low and high values in the range of 0.75 $(\times 10^3) - 2.51$ $(\times 10^3)$.

In the healed wound group, the graph shows an increase in S_tO_2 level during the early healing stage, whereby the wound were presumed to be in the epithelialization stage. This trend is especially apparent among positive healing wound (Subjects 001 and 002) with mean S_tO_2 that reached peak values (approximately 70 % and above) during the vascularization stage. A subsequent decrease in S_tO_2 was observed during the early stage of granulation. However these values continued to increase as the healing progressed until the wound is suspected to enter the maturation phase. The results of Subject 003, however, showed a slightly lower S_tO_2 of <70 % during the early stage following a post-Chopart amputation. Although the presence of infection was not reported, the physical changes of the wound were apparent as the perimeter size continued to increase six months into assessment. Nevertheless, a consistent mean S_tO_2 measuring above 77 % was reported for the wound, indicating a functioning arterial vasomotion at the investigated site. The subject was discharged from follow-up following physician's inspection of wound that showed progressive healing and evident reduction in wound perimeter. On the contrary, the S_tO_2 level observed in the impaired healing wound group showed an inconsistent trend with values fluctuating between below 50 % to above 70 % throughout the entire investigation period.

The results in Fig. 6 revealed a higher mean τ of 1.32 ± 0.54 $(\times 10^3)$ in the positive healing group as compared its counterpart group, with a mean τ of 1.30 ± 0.57 $(\times 10^3)$. This indicates a fairly small difference between the compared wound groups, with an overall low τ range for both groups of data. Likewise, the result revealed a higher mean S_tO_2 of 69.36 ± 8.59 % in the positive healing group as compared to the impaired healing group (S_tO_2 of 67.43 ± 9.72 %). An independent samples t-test revealed no statistically significant difference between the two groups of data, with a significant value of $p = 0.909$ and $p = 0.512$ calculated for mean τ and S_tO_2 values, respectively.

To investigate the microcirculatory performance associated with wound healing, data of the healthy control group under arterial blood occlusion condition were included for comparison with that from DFU subjects. This was considering the mean S_tO_2 and blood perfusion values during occlusion that was found to be in a close range to that observed in the DFU subjects in Fig. 4. Fig. 7 showed the number of data points in percent (in each group) associated with two specific clusters namely data points with low values (i.e. $\tau < 1.5$ $(\times 10^3)$ and $S_tO_2 < 70$ % indicated by red bars) and the remaining data points with high values (i.e. $\tau \geq 1.5$ (10^3) and $S_tO_2 \geq 70$ % indicated by blue bars).

In this study a total number of 59 data were collected from both the DFU investigation groups (positive healing ($N = 16$), impaired healing ($N = 28$)) and healthy control

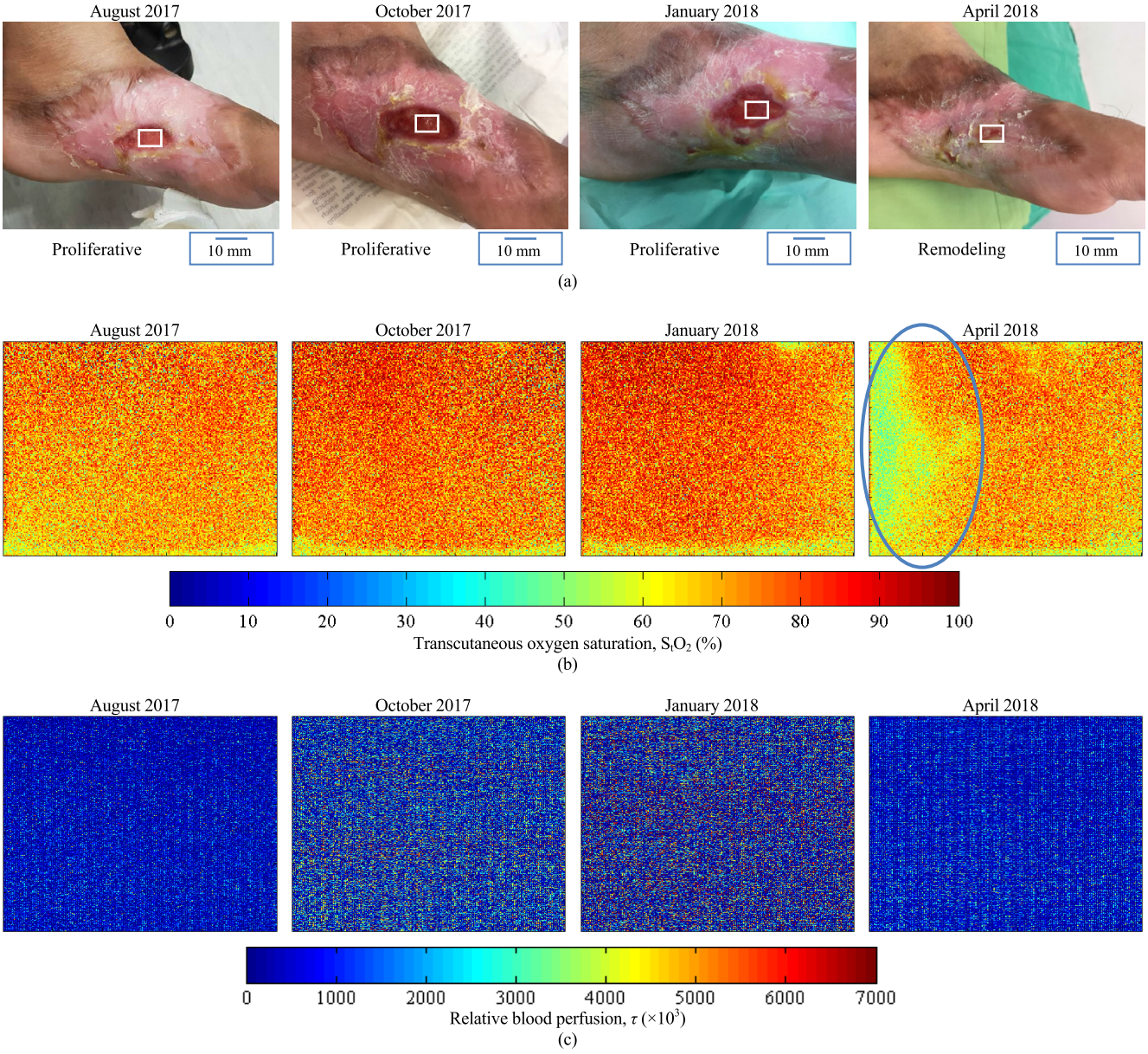

FIGURE 5. **(a) Changes in S_tO_2, and blood flow perfusion, τ, in a positive healing DFU. Measurements were recorded for a period of nine months. The level of (b) S_tO_2 and (c) τ of the imaged region is represented by the color bar below the maps.**

group (N = 15). The S_tO_2 and blood perfusion data of the control group were set as the benchmarks in this study. An investigation of these results showed that the number of data with low readings is relatively high among the impaired healing as compared to the control and healed wound groups. Approximately 53.57 % (N = 15) of total number of data from the impaired healing wound group were observed to have low τ and S_tO_2 values. The smaller number of low values data (N = 6) that falls below the selected threshold values observed among the healed group was expected considering these values were mostly for measurements collected on the day subjects were discharged. This drop in S_tO_2 is likely due to the reduced reactive oxygen series (ROS) production in healed wounds.

IV. DISCUSSION

This study explored the application of a laser speckle integrated multispectral imaging system for *in-vivo* assessment of diabetic wound healing. The results from this study were correlated with clinical inspection. This is with the aim of proposing quantitative measurement of microcirculatory performances for prediction of healing outcome, and to evaluate effectiveness of prescribed treatments. In agreement with the hypothesis of this study that optimal blood perfusion and tissue oxygen are necessary to warrant progressive healing, Fig. 6 showed an evident decrease in wound perimeter among four subjects (Subjects 001, 002, 003 and 004), while the investigated microcirculatory parameters fluctuate throughout this study in impaired healing group (Subjects

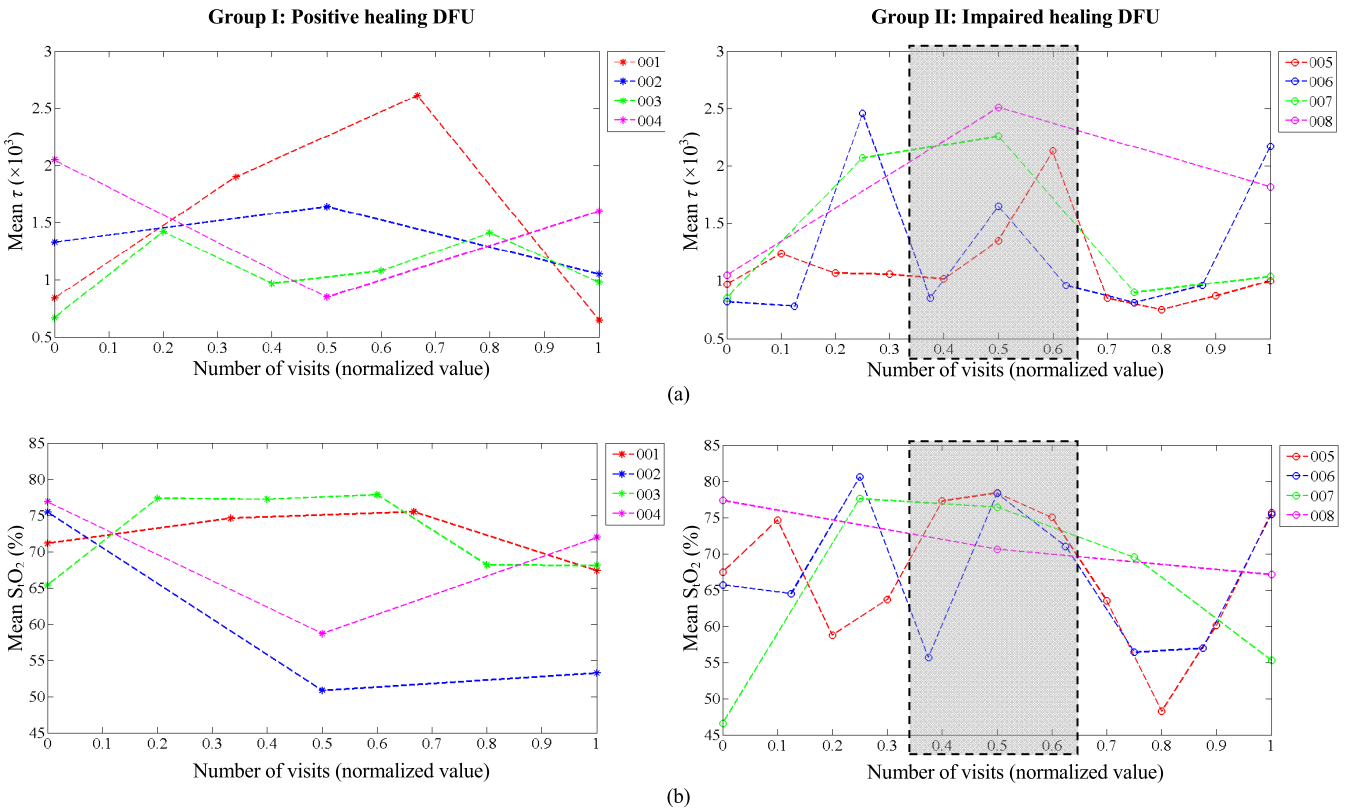

FIGURE 6. Changes in (a) mean blood perfusion, τ, and (b) transcutaneous tissue oxygenation, S_tO_2, of (left) positive healing diabetic wounds and (right) impaired healing diabetic wounds.

005, 006, 007 and 008). This is expected to be common in chronic wounds associated with diabetes mellitus and peripheral vascular diseases as the wounds do not undergo timely healing and the healing period could extend up to one year or more. Some subjects may experience oscillating wound blood perfusion and tissue oxygen as the ulcer progressed. An example of this was observed in Subject 004 in Fig. 6. In the first measurement taken one month into wound treatment, the S_tO_2 and τ values were recorded as the highest among all the visits at $76.89 \pm 2.28\,\%$ and $2.05 \pm 0.28\,(\times 10^3)$, respectively. Although a reduction in wound size was notable on the second visit, the measurements recorded a drastic drop in S_tO_2 values to $58.68 \pm 1.48\,\%$ and τ values to $0.85 \pm 0.25\,(\times 10^3)$. The wound appeared to be dehydrated when assessed by medical professionals during the visit with dusky edges indicating hypoxia. The ongoing treatment was substituted with hydrofiber wound dressing and oral hypoglycemic agents following the patient's adverse reaction to Cefuroxime medication. The measurement taken on the final visit revealed a mean S_tO_2 and τ that measured above $70\,\%$ and $1.5\,(\times 10)^3$, respectively. The subject was discharged following progressive healing and evidence of contraction in the ulcer.

Contrary to the trend observed among the positive healing group, the high blood perfusion and tissue oxygen does not guarantee a positive healing progress as these values could drop rapidly in between the investigated period, depending on how well the diabetic patient manages his or her wound. The fluctuation in microcirculatory changes observed in chronic wound could potentially be the reason for the delay in regeneration of new tissue, hence impeding wound healing. Measurement from Subject 005 in Fig. 6 is one such example. Initial measurement of the wound showed $S_tO_2 = 67.46 \pm 1.24\,\%$ and $\tau = 0.97 \pm 0.18\,(\times 10^3)$, with presence of cellulitis at the shin when inspected by the physician. The initial wound size was measured as $100\,\text{mm} \times 30\,\text{mm}$ with a depth of <10 mm. Despite the ulcer being treated with Dermacyn and Aquacel wound dressings to reduce exudation in wound and promote a moist surrounding, it did not show any noteworthy changes throughout the period of this study. This can be referred to the results in Fig. 6, whereby measurements from the first to fourth visit are observed to fluctuate with S_tO_2 values that ranged between $55\,\%$ and $80\,\%$, while τ values are between $0.95\,(\times 10^3)$ and $1.25\,(\times 10^3)$. Changes in medication were made on the fourth visit with the prescription of Methylcobalamin, a form of Vitamin B commonly used for restoration of red blood cells in patients with anemia and neuropathy. This saw an improvement in tissue oxygenation and perfusion in the following visits (Visit 5 – Visit 7) as highlighted in the grey region. Nevertheless, this study noted a drastic drop in values starting from the eighth visit of this subject, with the lowest S_tO_2 and τ values recorded as $48.25 \pm 6.14\,\%$ and $0.75 \pm 0.19\,(\times 10^3)$, respectively, on the ninth visit. The final measurement, taken after

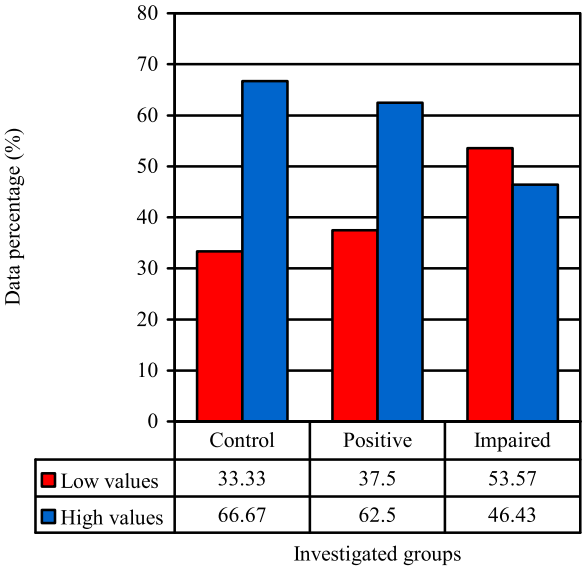

FIGURE 7. Percent number of data points with two different mean blood perfusion, τ, and tissue oxygen, S_tO_2, level sets. The thresholds are set as $S_tO_2 = 70$ % and $\tau = 1.5$ ($\times 10^3$). The red bar indicates number of data points with S_tO_2 and τ values lower than the threshold limits. Otherwise is true for the blue bar.

19 months from the first measurement, shows an S_tO_2 reading of 75.71 ± 2.28 % and τ value of $1.001.00 \pm 0.25$ $(\times 10^3)$, with the ulcer size reduced to 80 mm $\times$ 30 mm. This could be due to improper DFU management in Subject 005, which includes poor adherences to lifestyle, hygiene awareness and inappropriate footwear leading to abnormal loading of the plantar of the foot. This was confirmed by medical staff after inspection of foot condition. In addition musculoskeletal examination on this individual showed development of claw foot, which lead to formation of calluses, and dry skin with cracks and fissures around the ulcer. These neuropathic symptoms, alongside inadequate blood glucose control, are considered to be the main factors that could lead to reduced skin blood flow, thickening of vascular basement membrane and endothelial capillary in this patient [37], [38].

Unlike the high mean τ values observed among healthy control group at rest in Fig. 4(a), the blood perfusion range in diabetic wound was not significantly different from that observed in the healthy control group under ischemic condition. Specifically, these results support the previous findings in [39] that peripheral arterial disease can be characterized as the occlusion of artery or claudication in the lower extremity. The blood perfusion value in the lower tail of its distribution is the major impediment to reduced tissue oxygenation. The former is often associated with the thickening of capillary wall and fibrin deposition found in peripheral arterial and vascular diseases [40]. Patients with DFU commonly suffer from cyclic intervals of ischemia and poor perfusion in the lower extremity [39].

The normalized results in Fig. 6 and Fig. 7 revealed an overall higher mean blood perfusion and tissue oxygen level in the healed than the impaired wound group. This is, in particular prior to wound reepithelialization. It was found that the S_tO_2 level in wound gradually decreased as the wound entered maturation phase, denoting a stabilized immune system and regulated angiogenesis to improve scarring in skin during wound closure [41]. On the contrary, the fluctuating blood perfusion and tissue oxygen levels observed among the impaired healing group in Fig. 6 is a possible reason for the delay in regeneration of new tissue and wound to be completely healed. This fluctuating hypoxia may lead to cellular demise, and hence amputation of the affected part [42]. A further inspection into the medical history of these patients revealed other factors such age, obesity and poor-glycemic control, which may also be the risk-factors of diabetes-related neuropathy that affect the healing progress [43].

This study addresses the ongoing issue on the inter- and intra-observer variability in the grading of diabetic wounds (between categories Wagner's Grade 2 and 3) using tissue oxygenation and perfusion as its indicators. The employed approach combining laser speckle and reflectance spectroscopy is shown to be promising for examination of wound healing status without the use of tracers. Since most of these wounds were not examined starting from their early inflammatory phase, there remains a gap in understanding the progression and correlation between the blood flow and tissue oxygenation level of diabetic wounds from inflammation to the maturation phase.

Due to the variability in the stages of wound healing when the investigation subjects mentioned above were first recruited, physiological changes in DFU starting from metastasis to maturation phase remains to be further explored. In addition, while having more data increases certainty of the system's performance, this was not viable in the current study due to the limited study center and duration approved by ethical committees. Future works would suggest multi-center trials for better evaluation of the microcirculation performance of DFU patients with a diverse range of age categories and regular clinical visits for each subject.

Besides this, this work also recommends further improvement in hardware design. This included the aperture size that controls the exposure of the image. Although no optimal size is sought in this work, a detector aperture size of approximately 1/10 of the average diameter of a speckle is recommended in [44] to achieve the best result. This, however, is arguably impossible in practice as reducing the aperture size any further will unnecessarily limit the FOV and restrict the amount of light detected by the camera. Even though a high dynamic range camera with shutter speed control would compensate for the loss, this is at the cost of higher expenditure. Another option is the use of a high intensity laser source and polarizing filters to ensure only diffused light is detected and for improved signal to noise performance.

In this work, prediction of tissue oxygen saturation and perfusion is by using the EMLB and laser speckle contrast model that involved an extensive iterative fitting procedure. This approach not only demands high storage capacity, but is also time-consuming. The next line of this research is to

explore computer-based technologies such as artificial intelligence technique for real-time prediction.

In conclusion, this research is a multi-disciplinary work involving both clinical aspects of DFU (i.e. measurement of blood flow and tissue oxygenation) and instrumentation and software model fitting. The laser speckle integrated multispectral imaging system is the first known system to integrate laser speckle and reflectance spectroscopy technique for simultaneous imaging of blood flow perfusion and tissue oxygenation. This is, to the authors' knowledge, the first work to investigate blood flow perfusion using a laser wavelength of 650 nm, and to use wavelength range of $530 - 570$ nm for multispectral imaging of skin oximetry.

V. CONCLUSION

The results from this study suggested that a mean S_tO_2 of at least 70 % and blood perfusion value of at least $1.5\ (\times 10^3)$ are vital to ensure progressive healing. This research also noted a significantly low tissue perfusion and oxygenation level in the DFU subjects, which values are similar to that observed in the healthy control group during occlusion. This supported the previous findings on ischemia and possible risk of peripheral arterial disease in the lower extremity of diabetic patients. The mean S_tO_2 in the positive healing wound group was slightly higher than that of impaired healing with an absolute mean difference of 1.93 %. Likewise, the mean τ in positive healing wound group was slightly higher than the impaired healing wound group with an absolute mean difference of $0.02\ (\times 10^3)$. These results further support the hypothesis of this study, whereby high tissue oxygenation and perfusion levels are pivotal to ensure progressive wound healing. The inclusion of tissue oxygen and relative blood perfusion parameters in this research was of great importance for discussing cut-off points of the healing range in diabetic wounds. Therefore, if these data were used to predict diabetic wound outcome, necessary measures and actions can be taken to overcome the delays in healing progress.

ACKNOWLEDGMENT

The authors would like to thank all the medical staff from the orthopedic department of Hospital Sultanah Nora Ismail, Batu Pahat for their help during data collection. They would also like to thank the Director General of the Ministry of Health Malaysia for his permission to publish this article.

REFERENCES

[1] N. H. Cho, J. E. Shaw, S. Karuranga, Y. Huang, J. D. da Rocha Fernandes, A. W. Ohlrogge, and B. Malanda, "IDF diabetes atlas: Global estimates of diabetes prevalence for 2017 and projections for 2045," *Diabetes Res. Clin. Pract.*, vol. 138, pp. 271–281, Apr. 2018.

[2] L. Guariguata, D. R. Whiting, I. Hambleton, J. Beagley, U. Linnenkamp, and J. E. Shaw, "Global estimates of diabetes prevalence for 2013 and projections for 2035," *Diabetes Res. Clin. Pract.*, vol. 103, no. 2, pp. 137–149, Feb. 2014.

[3] N. S. Raja, "Microbiology of diabetic foot infections in a teaching hospital in Malaysia: A retrospective study of 194 cases," *J. Microbiol. Immunol. Infection*, vol. 40, p. 39, Feb. 2007.

[4] Z. Saringat, A. Mustapha, R. D. R. Saedudin, and N. A. Samsudin, "Comparative analysis of classification algorithms for chronic kidney disease diagnosis," *Bull. Electr. Eng. Informat.*, vol. 8, no. 4, pp. 1496–1501, Dec. 2019.

[5] T. Purwaningsih and B. Machmud, "Influence of overweight and obesity on the diabetes in the world on adult people using spatial regression," *Int. J. Adv. Intell. Inform.*, vol. 2, no. 3, pp. 149–156, 2016.

[6] K. Bakker, J. Apelqvist, B. A. Lipsky, J. J. Van Netten, and N. C. Schaper, "The 2015 IWGDF guidance documents on prevention and management of foot problems in diabetes: Development of an evidence-based global consensus," *Diabetes/Metabolism Res. Rev.*, vol. 32, pp. 2–6, Jan. 2016.

[7] S. Wang, Q. Zhang, W. Huang, H. Tian, J. Hu, Y. Cheng, and Y. Peng, "A new smart mobile system for chronic wound care management," *IEEE Access*, vol. 6, pp. 52355–52365, 2018.

[8] A. Khalil, M. Elmogy, M. Ghazal, C. Burns, and A. El-Baz, "Chronic wound healing assessment system based on different features modalities and non-negative matrix factorization (NMF) feature reduction," *IEEE Access*, vol. 7, pp. 80110–80121, 2019.

[9] Y. Wang, Y. Zhan, L. M. Harris, S. Khan, and J. Xia, "A portable three-dimensional photoacoustic tomography system for imaging of chronic foot ulcers," *Quant. Imag. Med. Surg.*, vol. 9, p. 799, May 2019.

[10] C. Lauri, A. W. J. M. Glaudemans, G. Campagna, Z. Keidar, M. Muchnik Kurash, S. Georga, G. Arsos, E. Noriega-Álvarez, G. Argento, T. C. Kwee, R. H. J. A. Slart, and A. Signore, "Comparison of white blood cell scintigraphy, FDG PET/CT and MRI in suspected diabetic foot infection: Results of a large retrospective multicenter study," *J. Clin. Med.*, vol. 9, no. 6, p. 1645, May 2020.

[11] S. Vaidyanathan, C. N. Patel, A. F. Scarsbrook, and F. U. Chowdhury, "FDG PET/CT in infection and inflammation—Current and emerging clinical applications," *Clin. Radiol.*, vol. 70, no. 7, pp. 787–800, Jul. 2015.

[12] S. Eser Sanverdi, B. Ergen, and A. Oznur, "Current challenges in imaging of the diabetic foot," *Diabetic Foot Ankle*, vol. 3, no. 1, p. 18754, Jan. 2012.

[13] J. Yao, K. I. Maslov, Y. Shi, L. A. Taber, and L. V. Wang, "*In vivo* photoacoustic imaging of transverse blood flow by using Doppler broadening of bandwidth," *Opt. Lett.*, vol. 35, no. 9, pp. 1419–1421, 2010.

[14] S. Wang, Y. Zhao, and Y. Xu, "Recent advances in applications of multimodal ultrasound-guided photoacoustic imaging technology," *Vis. Comput. Ind., Biomed., Art*, vol. 3, no. 1, pp. 1–12, Dec. 2020.

[15] A. Garcia-Uribe, T. N. Erpelding, A. Krumholz, H. Ke, K. Maslov, C. Appleton, J. A. Margenthaler, and L. V. Wang, "Dual-modality photoacoustic and ultrasound imaging system for noninvasive sentinel lymph node detection in patients with breast cancer," *Sci. Rep.*, vol. 5, no. 1, p. 15748, Dec. 2015.

[16] K. Istiaque Ahmed, M. Hadi Habaebi, and M. R. Islam, "Smartphone aided real-time blood vein detection system," *Bull. Electr. Eng. Informat.*, vol. 8, no. 3, pp. 1096–1107, Sep. 2019.

[17] M. Li, Y. Tang, and J. Yao, "Photoacoustic tomography of blood oxygenation: A mini review," *Photoacoustics*, vol. 10, pp. 65–73, Jun. 2018.

[18] C. Shiba, T. Shiba, M. Takahashi, T. Matsumoto, and Y. Hori, "Relationship between glycosylated hemoglobin A1c and ocular circulation by laser speckle flowgraphy in patients with/without diabetes mellitus," *Graefe's Arch. Clin. Experim. Ophthalmol.*, vol. 254, no. 9, pp. 1801–1809, Sep. 2016.

[19] S. C. Gnyawali, K. Blum, D. Pal, S. Ghatak, S. Khanna, S. Roy, and C. K. Sen, "Retooling laser speckle contrast analysis algorithm to enhance non-invasive high resolution laser speckle functional imaging of cutaneous microcirculation," *Sci. Rep.*, vol. 7, no. 1, p. 41048, Feb. 2017.

[20] N. K. Shaydyuk and T. Cleland, "Biometric identification via retina scanning with liveness detection using speckle contrast imaging," in *Proc. IEEE Int. Carnahan Conf. Secur. Technol. (ICCST)*, Oct. 2016, pp. 1–5.

[21] A. Huong, S. Philimon, and X. Ngu, "Multispectral imaging of acute wound tissue oxygenation," *J. Innov. Opt. Health Sci.*, vol. 10, no. 3, May 2017, Art. no. 1750004.

[22] W.-M. Liu, C.-L. Chen, L.-Y. Chang, S.-C. Pong, and H.-M. Chen, "Multimodal and multispectral imaging for chronic pressure ulcer assessment," in *Proc. 2nd Int. Conf. Biomed. Signal Image Process. (ICBIP)*, 2017, pp. 47–52.

[23] R. B. Saager, M. L. Baldado, R. A. Rowland, K. M. Kelly, and A. J. Durkin, "Method using *in vivo* quantitative spectroscopy to guide design and optimization of low-cost, compact clinical imaging devices: Emulation and evaluation of multispectral imaging systems," *J. Biomed. Opt.*, vol. 23, Apr. 2018, Art. no. 046002.

[24] K. Nakano, R. Hirofuji, T. Ohnishi, M. Hauta-Kasari, I. Nishidate, and H. Haneishi, "RGB camera-based imaging of oxygen saturation and hemoglobin concentration in ocular fundus," *IEEE Access*, vol. 7, pp. 56469–56479, 2019.
[25] L. E. Lindley, O. Stojadinovic, I. Pastar, and M. Tomic-Canic, "Biology and biomarkers for wound healing," *Plastic Reconstructive Surg.*, vol. 138, no. 3, p. 18S, 2016.
[26] D. André-Lévigne, A. Modarressi, R. Pignel, M. Bochaton-Piallat, and B. Pittet-Cuénod, "Hyperbaric oxygen therapy promotes wound repair in ischemic and hyperglycemic conditions, increasing tissue perfusion and collagen deposition," *Wound Repair Regener.*, vol. 24, no. 6, pp. 954–965, Nov. 2016.
[27] L. M. Richards, S. S. Kazmi, J. L. Davis, K. E. Olin, and A. K. Dunn, "Low-cost laser speckle contrast imaging of blood flow using a Webcam," *Biomed. Opt. Exp.*, vol. 4, pp. 2269–2283, Oct. 2013.
[28] I. V. Meglinski and S. J. Matcher, "Quantitative assessment of skin layers absorption and skin reflectance spectra simulation in the visible and near-infrared spectral regions," *Physiol. Meas.*, vol. 23, no. 4, p. 741, 2002.
[29] W. J. Tom, A. Ponticorvo, and A. K. Dunn, "Efficient processing of laser speckle contrast images," *IEEE Trans. Med. Imag.*, vol. 27, no. 12, pp. 1728–1738, Dec. 2008.
[30] A. Dunn and W. J. Tom, "Methods of producing laser speckle contrast images," U.S. Patent 8 823 790, Sep. 2, 2014.
[31] A. F. Fercher and J. D. Briers, "Flow visualization by means of single-exposure speckle photography," *Opt. Commun.*, vol. 37, no. 5, pp. 326–330, Jun. 1981.
[32] D. Briers, D. D. Duncan, E. Hirst, S. J. Kirkpatrick, M. Larsson, W. Steenbergen, T. Stromberg, and O. B. Thompson, "Laser speckle contrast imaging: Theoretical and practical limitations," *J. Biomed. Opt.*, vol. 18, no. 6, Jun. 2013, Art. no. 066018.
[33] A. Huong and X. Ngu, "The application of extended modified lambert beer model for measurement of blood carboxyhemoglobin and oxyhemoglobin saturation," *J. Innov. Opt. Health Sci.*, vol. 07, no. 03, May 2014, Art. no. 1450026.
[34] R. N. Pittman and B. R. Duling, "A new method for the measurement of percent oxyhemoglobin," *J. Appl. Physiol.*, vol. 38, no. 2, pp. 315–320, Feb. 1975.
[35] J. C. Lagarias, J. A. Reeds, M. H. Wright, and P. E. Wright, "Convergence properties of the nelder-mead simplex method in low dimensions," *SIAM J. Optim.*, vol. 9, no. 1, pp. 112–147, Jan. 1998.
[36] A. K. C. Huong, "Spectroscopic analysis of scattering media via different quantification techniques," M.S. thesis, Dept. Elect. Electron. Eng., Univ. Nottingham, Nottingham, U.K., 2012.
[37] E. Everett and N. Mathioudakis, "Update on management of diabetic foot ulcers," *Ann. New York Acad. Sci.*, vol. 1411, no. 1, p. 153, 2018.
[38] B. A. Lipsky, J. Aragón-Sánchez, M. Diggle, J. Embil, S. Kono, L. Lavery, É. Senneville, V. Urbančič-Rovan, S. Van Asten, and E. J. G. Peters, "IWGDF guidance on the diagnosis and management of foot infections in persons with diabetes," *Diabetes/Metabolism Res. Rev.*, vol. 32, pp. 45–74, Jan. 2016.
[39] N. M. Hamburg and M. A. Creager, "Pathophysiology of intermittent claudication in peripheral artery disease," *Circulat. J.*, vol. 81, no. 3, pp. 281–289, 2017.
[40] M. Roustit, J. Loader, D. Baltzis, W. Zhao, and A. Veves, "Microvascular changes in the diabetic foot," in *The Diabetic Foot*. Cham, Switzerland: Springer, 2018, pp. 173–188.
[41] L. A. DiPietro, "Angiogenesis and wound repair: When enough is enough," *J. Leukocyte Biol.*, vol. 100, no. 5, pp. 979–984, Nov. 2016.
[42] R. Chawla, A. Chawla, and S. Jaggi, "Microvasular and macrovascular complications in diabetes mellitus: Distinct or continuum?" *Indian J. Endocrinology Metabolism*, vol. 20, no. 4, p. 546, 2016.
[43] S. T. Andersen, D. R. Witte, J. Fleischer, H. Andersen, T. Lauritzen, M. E. Jørgensen, T. S. Jensen, R. Pop-Busui, and M. Charles, "Risk factors for the presence and progression of cardiovascular autonomic neuropathy in type 2 diabetes: Addition-Denmark," *Diabetes Care*, vol. 41, no. 12, pp. 2586–2594, Dec. 2018.
[44] J. D. Briers, "Laser Doppler, speckle and related techniques for blood perfusion mapping and imaging," *Physiol. Meas.*, vol. 22, no. 4, pp. R35–R66, Nov. 2001.

SHEENA PUNAI PHILIMON (Member, IEEE) was born in Sarawak, Malaysia, in 1990. She received the B.Eng. degree in electronic engineering and the master's degree in electrical engineering from Universiti Tun Hussein Onn Malaysia (UTHM), in 2014 and 2016, respectively, and the Ph.D. degree from the Department of Electronic Engineering, Faculty of Electrical and Electronic Engineering, UTHM, in 2020. She is currently a Lecturer with the School of Information and Communications Technology, Faculty of Engineering, Computing and Science, Swinburne University of Technology at Sarawak. Her research interests include biomedical optics, spectroscopy imaging, and laser speckle contrast imaging.

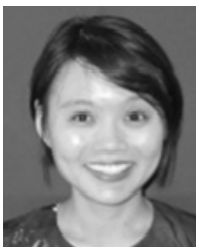

AUDREY KAH CHING HUONG (Senior Member, IEEE) was born in Sarawak, Malaysia, in 1981. She received the B.Eng. degree in medical electronics from Universiti Tun Universiti Tun Hussein Onn Malaysia (UTHM), in 2005, and the Ph.D. degree in biomedical optics and imaging from the University of Nottingham, in 2012. She is currently a Principal Researcher with the Biomedical Engineering Modelling and Simulation Research Group (BIOMEMS) and an Associate Professor with the Department of Electronic Engineering, Faculty of Electrical and Electronic Engineering, UTHM. Her research interests include biomedical optics, polarization microscopy, and spectroscopy imaging.